JACS
JOURNAL OF THE AMERICAN CHEMICAL SOCIETY

ARTICLE

pubs.acs.org/JACS

Axial-Bundle Phases − New Modes of 2D, 3D, and Helical Columnar Self-Assembly in Liquid Crystalline Phases of Bolaamphiphiles with Swallow Tail Lateral Chains

Marko Prehm,[†] Feng Liu,[‡] Xiangbing Zeng,[‡] Goran Ungar,[*,‡,§] and Carsten Tschierske[*,†]

[†]Organic Chemistry, Institute of Chemistry, Martin-Luther-University Halle-Wittenberg, Kurt-Mothes-Strasse 2, D-06120 Halle, Germany

[‡]Department of Materials Science and Engineering, University of Sheffield, Mappin Street, Sheffield S13JD, United Kingdom

[§]WCU Program Chemical Convergence for Energy & Environment, School of Chemical and Biological Engineering, Seoul National University, Seoul, Korea

Supporting Information

ABSTRACT: Two series of polyphilic molecules composed of a rigid and linear *p*-terphenyl core, terminated at both ends with polar glycerol groups capable of hydrogen bonding, and two branched swallow tail-type lateral chains, composed of a fluorinated and a nonfluorinated branch or two fluorinated branches, were synthesized and investigated by differential scanning calorimetry, polarizing microscopy, and X-ray diffraction (XRD) with respect to their self-assembly in thermotropic liquid crystalline (LC) phases. Hexagonal columnar phases were formed by all molecules, at least at the highest temperature. In these phases the columns are composed of a core of aromatic rods and an aliphatic shell. The aromatic rods form bundles which are rotationally averaged and lie parallel to the column long axis. This unique organization is proven by different optical and XRD methods. The aromatic and glycerol groups inside the rod bundles are segregated into alternating segments. Depending on temperature and molecular structure, long-range intercolumnar correlation of this periodicity could take place, leading to a 3D-ordered LC phase with rhombohedral $R\bar{3}m$ symmetry. The bundles are embedded in the matrix of the lateral chains, which is divided into fluoroalkyl- and aliphatic-rich regions. In the 2D columnar phase the fluorinated regions take the form of either straight columns running along the edges of the hexagonal Voronoi cells or, for compounds with a higher degree of fluorination, fuse to a hexagonal honeycomb enclosing the aromatic cores. In the $R\bar{3}m$ phase the fluorine-rich chains are preferentially found along right- and left-handed helices wound around the 3_1 screw axes between the main aromatic columns.

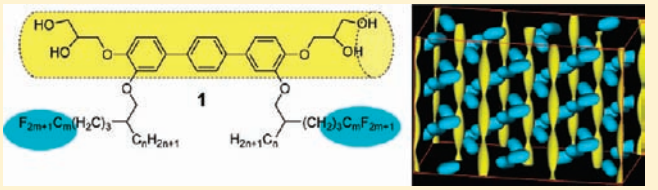

INTRODUCTION

The combination of mobility and order in soft self-assembled superstructures[1] is an indispensable feature of numerous self-assembled structures that form the basis of both life and numerous technical devices.[2] Liquid crystalline (LC) phases are prototypical self-assembled systems combining long-range order and mobility.[3−5] The discovery that disk-like molecules can organize into LC phases in which the molecules stack up in columns (Figure 1)[6] initiated intense activity in the field of columnar LC phases.[7] Especially the overlapping π-systems of aromatic disk-like molecules within the columns lead to interesting materials for molecular electronics and photovoltaics.[8,9] About 10 years after the discovery of discotic LC, it was shown by Malthete, Destrade, Levelut, and Tinh that rod-like (calamitic) molecules can also form columnar LC phases if two or three alkyl chains were attached at the ends of rod-like molecules.[10,11] Since then the concept of polycatenar mesogens[12] was extended to metallomesogens,[13] polymers,[14] hydrogen-bonded,[15] and ionic[16] LC systems. Besides linear alkyl chains, also branched chains (swallow tail chains)[17] and other bulky groups, such as strongly coiled chains (e.g., oligo(ethylene oxides), oligo(propylene oxides),[18] oligosiloxanes)[19] and fluorinated chains,[20] were attached in terminal position to calamitic or bent aromatic cores[21] to form columnar mesophases.[4,22−27]

Columnar LC phases formed by the rod-like molecules reported so far can be viewed as ribbon phases, i.e., layers sliced up into infinite ribbons in which the rod-like cores are perpendicular or tilted at a moderate angle with respect to the column long axis (Figure 1c).[10,11,28] Another, relatively new approach to columnar phases combines rod-like segments with terminal and lateral chains which are incompatible with each other. This concept of polyphilic T-shaped tectons provided a series of novel columnar LC phases described as honeycombs, where rod-like units form polygonal cylinder frames, and the flexible lateral chains fill the interior of the cylinder cells (Figure 1e).[29−31] With respect to the positions of rigid and flexible units, these mesophases are the inverse of those formed by disk-like molecules and

Received: November 9, 2010
Published: March 10, 2011

dx.doi.org/10.1021/ja110065r | J. Am. Chem. Soc. 2011, 133, 4906–4916

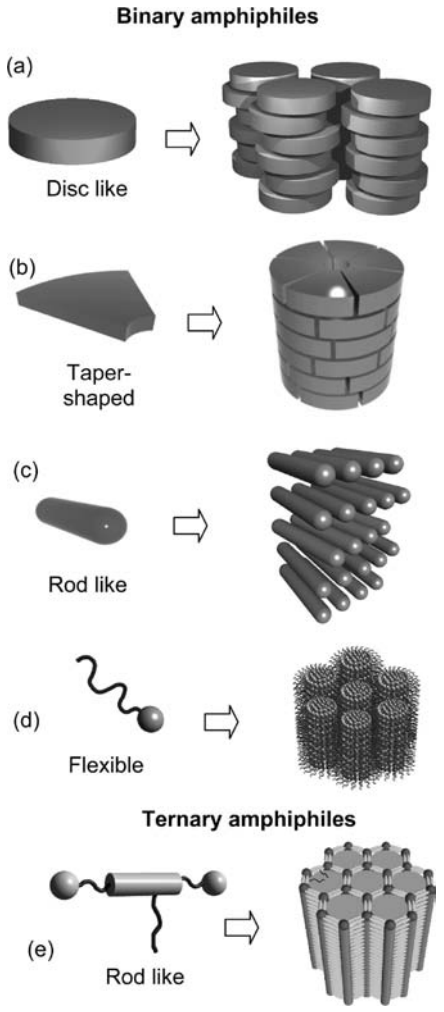

Figure 1. Major groups of columnar LC phases formed by different types of molecular building blocks.

previously reported rod-like molecules where the rigid segments occupy the center of the cells.

Here we report two modes of organization in columnar LCs where rod-like units form the interior rather than the periphery of the cells, but where, in contrast to previously reported columnar phases of polycatenars, the rod-like molecules lie parallel to the column axis in bundles. In one of them the columns are longitudinally uncorrelated, giving a true 2D hexagonal columnar phase, which was reported for only two examples in previous communications.[30f,32] The other one is a correlated type, giving a new rhombohedral $R\bar{3}m$ phase with 3D order.

The molecular alignment of the π-conjugated rods parallel to the columns is also in contrast to the columnar structures formed by discotic LC widely used for charge carrier materials.[8] In this way the structures reported herein provide the benefits of LC self-assembly (no grain boundaries, self-healing, directed alignment) also to rod-like materials with their intramolecular π-conjugation path parallel to the columns. Hence, the results could contribute to understanding and improving the self-assembly and alignment of π-conjugated oligomers and polymers representing another important class of charge carrier materials.[33]

Moreover, the continuum between the columns is divided into fluorous and aliphatic regions, whereby the fluorinated domains

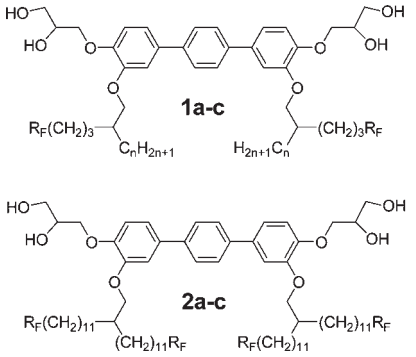

Comp.	n	R_F
1a	7	C_4F_9
1b	9	C_6F_{13}
1c	11	C_8F_{17}
2a	-	C_4F_9
2b	-	C_6F_{13}
2c	-	$C_{10}F_{21}$

assume the shape of either straight columns or helices. For compounds with a higher degree of fluorination, the fluorous columns fuse to a hexagonal honeycomb enclosing the aromatic columns. These new phase structures were obtained with specifically designed molecules, having branched (swallow tail) semiperfluorinated chains attached laterally to glycerol-terminated rigid rod-like *p*-terphenyl units. The role of the glycerol groups, attached at both ends, is to provide end-to-end linking of the rod-like cores by hydrogen bonding. Two swallow tail substituents were attached, with only one of the branches being fluorinated in compounds **1** and both branches fluorinated in compounds **2**.

RESULTS AND DISCUSSION

1. Synthesis. The synthesis (Scheme 1) starts with benzene 1,4-diboronic acid which is coupled in a Suzuki type reaction[34] with two equivalents of the acetonide protected glycerol functionalized arylbromide **A**.[35] In the obtained terphenyl derivative **B**, the benzyl groups were removed by catalytic hydrogenation, and the resulting *p*-terphenyldiol **C** was used for etherification reactions with semiperfluorinated and branched alkyl bromides

Scheme 1. Synthesis of compounds 1 and 2[a]

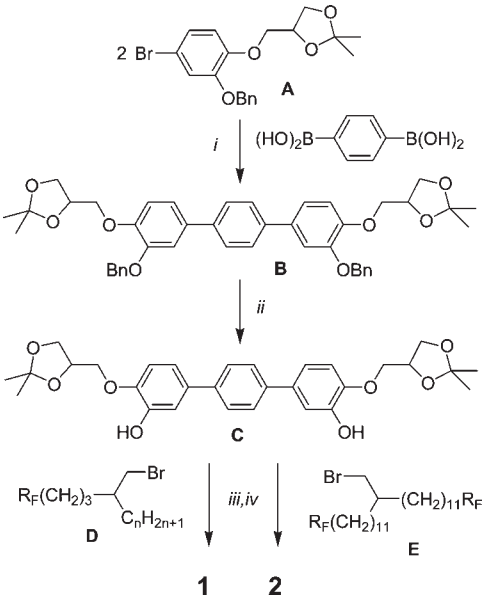

[a] Reagents and conditions: (i) $Pd[PPh_3]_4$, $NaHCO_3$, glyme, H_2O, reflux; (ii) H_2, Pd/C, EtOAc, 45 °C; (iii) K_2CO_3, DMF, 50-60 °C; (iv) HCl, MeOH, reflux.

dx.doi.org/10.1021/ja110065r |*J. Am. Chem. Soc.* 2011, 133, 4906–4916

Table 1. Mesophases, Phase Transitions, and Other Parameters of Compounds 1, Depending on the Size of the Lateral Chains[a]

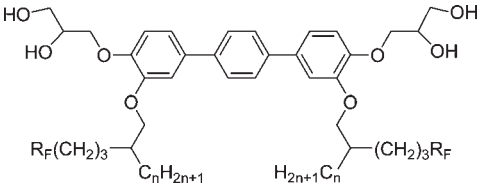

			T / °C				Lattice parameter/nm				
comp.	n	R_F	ΔH / kJ·mol^{-1}				a_{hex}	a_{hex}, c^b	f_R	f_{RF}	n_{cell}
1a	7	C_4F_9	Cr 103	$R\bar{3}m$	150 Col_{hex}	159 Iso	2.95	5.19, 2.27	0.64	0.22	10.4
			7.8		—	11.2					
1b[c]	9	C_6F_{13}	Cr 81	$R\bar{3}m$	130 Col_{hex}	154 Iso	3.11	5.45, 2.25	0.69	0.28	9.8
			21.3		—	7.8					
1c	11	C_8F_{17}	Cr 76	$R\bar{3}m$	125 Col_{hex}	156 Iso	3.32	5.87, 2.24	0.73	0.32	9.7
			31.3		—	8.0					

[a] Transition temperatures and enthalpy values (lower lines) were taken from first DSC heating curves (peak temperatures, 10 K min^{-1}); for DSC traces of compound **1a** and **1c** see Figures S1, Supporting Information and 8a, respectively; $R\bar{3}m$/Col_{hex} transitions were determined by temperature-dependent XRD; abbreviations: Cr = crystalline solid; Col_{hex} = hexagonal columnar LC phase; $R\bar{3}m$; correlated Col_{hex} phase with rhombohedral 3D-lattice; Iso = isotropic liquid; f_R = total volume fraction of the nonpolar lateral chains, including the fluorinated and aliphatic segments (calculated using crystal volume increments);[37] f_{RF} = volume fraction of the fluorinated part of the lateral chains only; n_{cell} number of molecules in a hypothetical "unit cell" of the Col_{hex} phase, calculated according to $n_{cell} = V_{cell}/V_{mol}$, where the volume of the "cell" (V_{cell}) is the product of the cell area and the molecular length $a^2 \times \sin(60°) \times 2.2$ nm, and the molecular volume (V_{mol}) is obtained from crystal volume increments, considering the reduced packing density in the LC state (for more details of calculations, see Table S10, Supporting Information). [b] Refers to the $R\bar{3}m$ phase. [c] Preliminary report, see ref 32.

Table 2. Mesophases, Phase Transitions, and Other Parameters of Compounds 2 Depending on the Length of the Fluorinated Segments[a]

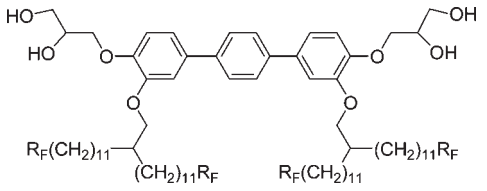

		T / °C							
comp.	R_F	ΔH / kJ·mol^{-1}				a / nm	f_R	f_{RF}	n_{cell}
2a	C_4F_9	Cr 83	M 97	Col_{hex}	161 Iso	3.68	0.78	0.27	9.9
		12.3	4.8		9.9				
2b	C_6F_{13}	Cr 83	Col_{hex}	175 Iso		3.89	0.80	0.35	9.8
		22.9		11.7					
2c	$C_{10}F_{21}$	Cr 122	Col_{hex}	191 Iso		4.49	0.84	0.47	10.7
		108.9		10.8					

[a] Transition temperatures and enthalpy values (lower lines) were taken from first DSC heating curves (peak temperatures, 10 K min^{-1}); for DSC traces of compound **2a** as representative example, see Figure S3, Supporting Information; abbreviations: M = unknown mesophase, for other abbreviations, see explanation in Table 1.

(**D**, **E**) in a Williamson ether synthesis to introduce the lateral chains. After purification of the acetonides the glycerol groups were deprotected, yielding compounds **1a**−**c** and **2a**−**c**.[36]

2. Mesomorphic Self-Assembly. The compounds were investigated by differential scanning calorimetry (DSC, DSC-7, Perkin-Elmer), polarizing microscopy (Optiphot 2, Nikon polarizing microscope in conjunction with a FP 82 HT heating stage, Mettler) and different X-ray diffraction (XRD) techniques, using powder samples and surface aligned samples. Investigations of surface aligned samples were performed using a 2D detector (HI-Star, Siemens). Uniform orientation was achieved by slowly cooling a drop of the compound on a glass surface. The X-ray beam was applied parallel to the substrate (exposure time: between 30 min and 3 h). For selected compounds, a synchrotron X-ray source was used for the investigation of the powder samples (beamline I22 at Diamond Light Source) and the surface aligned samples on silicon substrates by grazing incidence (GISAXS) (beamlines BM28−XMaS at ESRF, and I07 at diamond). Based on the powder data, electron density reconstruction was carried out. Details of the reconstruction process are described in Supporting Information. Transition temperatures, transition enthalpies and observed mesophases of compounds **1** and **2** are collated in Tables 1 and 2, respectively. All compounds show enantiotropic (thermodynamically stable) LC phases over broad temperature ranges.

*2.1. Hexagonal Columnar Phases of Compounds **1** and **2**.* The mesophases formed by compounds **1** and **2** are characterized by mosaic-like textures (Figure 2a) or by spherulitic textures as typical for columnar phases (Figure 2b). Homeotropically aligned samples (columns perpendicular to the surfaces) appear completely dark between crossed polarizers, indicating optical uniaxiality of the mesophases. The XRD patterns have a diffuse wide angle halo confirming the absence of crystalline order on the atomic scale (see Figures 3a and S6a, Supporting Information). The maximum of this diffuse scattering shifts with increasing degree of fluorination from $d \approx 2\pi/q = 0.50$ nm (compound **1a**) to 0.55 nm (compound **2c**). The d-values of the

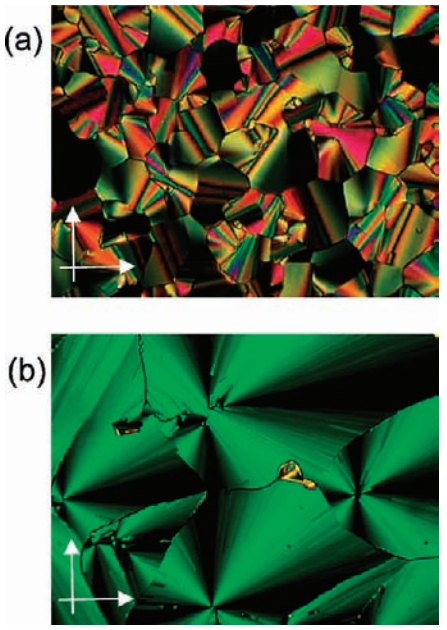

Figure 2. Typical textures of the Col_{hex} phases of compounds **1** and **2** as observed between crossed polarizers: (a) mosaic-like texture with pseudoisotropic areas of compound **1a** at T = 150 °C and (b) spherulitic texture of compound **1c** at T = 150 °C; directions of polarizer and analyzer are indicated by arrows.

small angle reflections have the ratio 1: $1/\sqrt{3}$: 1/2, characteristic of hexagonal symmetry, which is confirmed by diffraction patterns of surface aligned samples. Diffraction patterns of compound **2a**, as representative examples, are shown in Figure 3a and b (for more details see also Figures S2, S4, and S6 and Tables S1−S9, Supporting Information).

Enlarging the lateral chains (i.e., increasing f_R, see Tables 1 and 2) continuously increases the hexagonal lattice parameter from a_{hex} = 2.95 nm for compound **1a** (f_{RF} = 0.22) to a_{hex} = 4.49 nm for compound **2c** (f_{RF} = 0.47).[38] This continuous swelling is important for the interpretation of the structure of these Col_{hex} phases, as it excludes the possibility of a hexagonal honeycomb structure. In polygonal honeycombs, which are the most common structures in rod-like bolaamphiphiles with lateral chains (see Figure 1e),[30a,b] the lattice parameter is fixed within narrow limits by the length and the number of rod-like cores making up the circumference of a given polygon; significant expansion of the lattice would thus require a change of symmetry.[39,40] This is clearly not the case for the Col_{hex} phases of compounds **1** and **2**.

The electron density map reconstructed from the small-angle powder diffraction pattern of the Col_{hex} phase of compound **2a** is shown as an example in Figure 3c. Each column is characterized by a circular high electron density center (purple/blue), surrounded by a shell of lowest density (red). As the lowest electron density is provided by the aliphatic segments of the lateral chains, it is reasonable to assume that it is these segments that constitute the low-density ring surrounding the aromatic/glycerol central maximum. Furthermore, six electron density maxima are located at the vertices of the hexagonal Voronoi cell, and these are attributed to regions rich in fluorinated (C_4F_9) end groups. These small fluorinated segments tend to partially mix with aliphatic segments, hence the large areas of continuum at column boundaries with medium electron density (green/light blue).

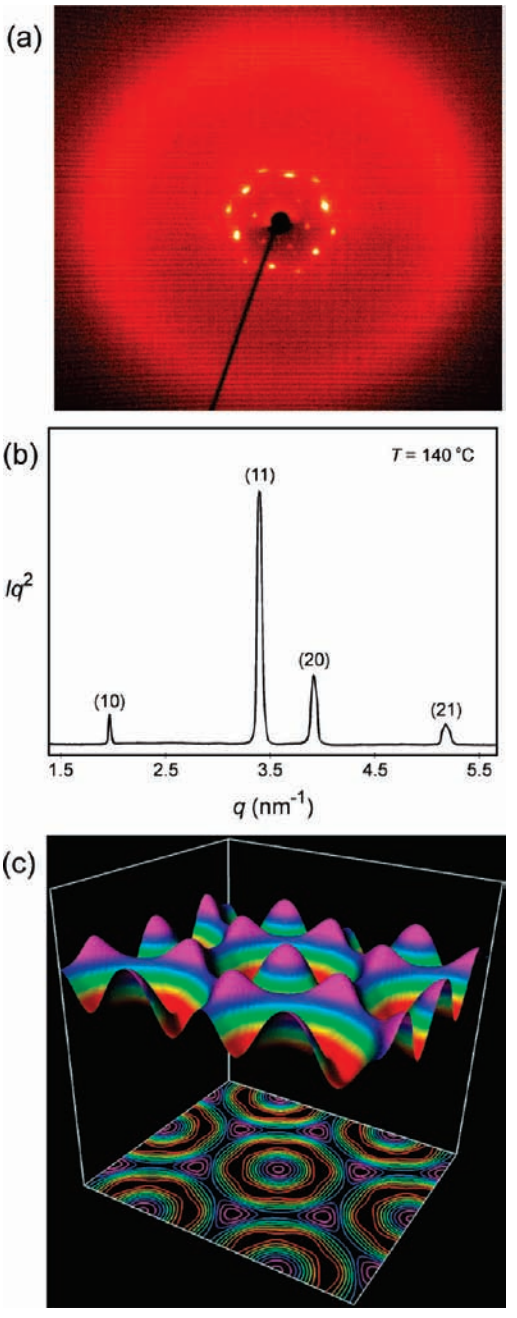

Figure 3. Col_{hex} phase of compound **2a**: (a) XRD pattern of a surface aligned sample at T = 143 °C (X-ray beam parallel to the surface); (b) small-angle X-ray scattering (SAXS) powder pattern at T = 140 °C; (c) surface-and-contour plot of electron density distribution in the plane normal to the column axis, reconstructed from diffraction pattern in (b).

Only at the vertices, which are difficult to reach by the aliphatic segments, a considerably higher concentration of electron-rich fluorinated chains is found.

In contrast to compounds **1c** and **2a**, in compound **2c**, which has the largest R_F segments, the electron-rich fluorinated columns are fused to form an uninterrupted hexagonal honeycomb around the core−shell columns (Figures 4b and 5d). The difference between the discrete fluorine-rich columns in compounds **1c** and **2a**, on the one hand, and the continuous fluorinated honeycomb in **2c** is illustrated schematically in Figure 11a and b (Section 2.2).

dx.doi.org/10.1021/ja110065r | *J. Am. Chem. Soc.* 2011, 133, 4906–4916

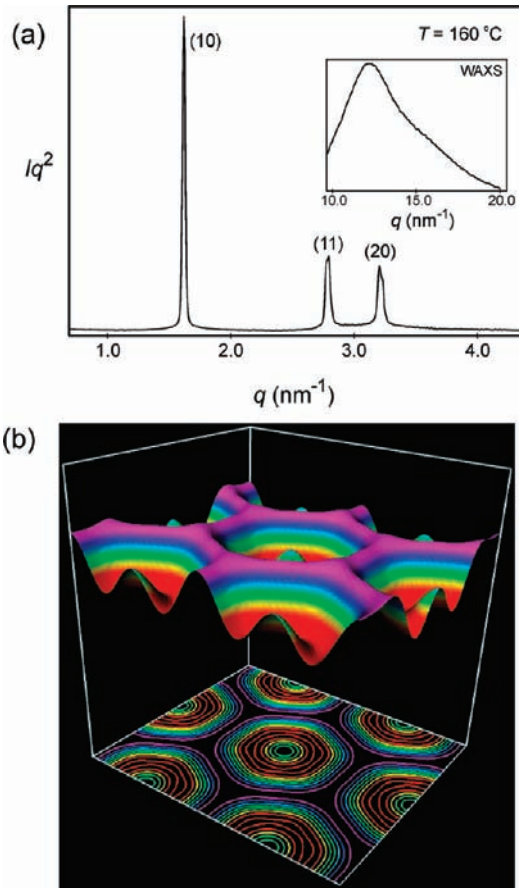

Figure 4. (a) Small angle XRD pattern of Col_{hex} phase of compound **2c** recorded at T = 160 °C (the inset shows the wide-angle region); (b) surface-and-contour plot of the electron density reconstructed from (a). Note that the electron densities are not directly comparable with those in Figure 3 as each map is scaled individually between red (lowest) and purple (highest).

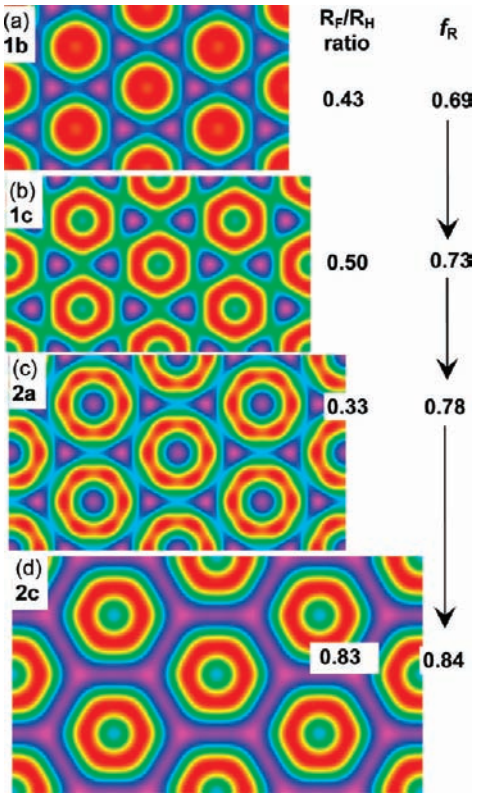

Figure 5. Comparison of electron density maps of the Col_{hex} phases of compounds (a) **1b**[32] and (b) **1c**, having only one fluorinated chain in each swallow tail (T = 140 °C), and (c) **2a** (T = 140 °C) and (d) **2c** (T = 160 °C), both latter compounds having two fluorinated branches in each swallow tail. The unit cell sizes are normalized to the same length scale. Note however that the electron densities are scaled individually, from red (lowest) to purple (highest) each. This is why, e.g., the column centers have different colors, although their electron densities are expected to be the same in all compounds; f_R = volume fraction of the lateral chains.

The maps of the Col_{hex} phase of compounds **1b** and **1c**, having only one fluorinated branch in each swallow tail, are shown in Figure 5a and b. In compound **1c** the high electron density regions of C_8F_{17} chains form separate columns at the vertices of the Voronoi cells. However, the relatively short and sparse C_6F_{13} groups in compound **1b** seem to mix with the alkyl groups resulting in a continuum at column periphery that has higher average electron density than the column core (Figure 5a). Indeed, calculation gives average electron densities of the terphenyl + glycerol region as 560 el/nm^3, as compared to 610 el/nm^3 for the mixed region of lateral chains. Figure 5c and d show 2D maps for compounds **2a** and **2c**, for comparison.

As shown in Figure 6, the aromatic cores of compounds **1** and **2** may lie either parallel (Figure 6b) or perpendicular (Figure 6a) to the column axis. The orientation of the aromatic core with respect to the columns was investigated by two methods.

Compound **2a** was doped with Disperse-red-1, (0.5 weight-%). Disperse-red-1 (Figure 7) is an anisometric (rod-like) and dichroic azo dye with the transition moment for the absorption at λ = 504 nm parallel to the molecular long axis.[41] Due to the polar groups at both ends of the azobenzene moiety, this dye has a bolaamphiphilic and rod-like structure, and hence, it should mix with and be parallel to the terphenyls. Between crossed polarizers the mixture shows a texture (see Figure 7a,) with homeotropically aligned regions (dark areas, columns perpendicular to the substrate surfaces) and regions with spherulitic texture where the columns form concentric rings which are predominantly parallel to the substrate surfaces. In Figure 7b the same region is shown but with parallel polarizers. Red color, indicating an alignment of the dye molecules with their long axis parallel to the substrate (i.e., with the conjugated π-system perpendicular to the direction of the light beam allowing maximal light absorption) is observed in the regions with spherulitic texture. The observation of less absorbing (yellow) areas in the homeotropically aligned regions indicates that chromophore and column axis coincide and that both are perpendicular to the surface. This excludes honeycomb-like or any other organization of the terphenyls perpendicular to the column axis (e.g., Figure 6a) and indicates that the aromatic cores of the host molecules **2a** are parallel to the columns, as shown in Figures 6b and 7c.

That the orientation of the aromatics is coaxial with the columns for all compounds **1** and **2** was additionally confirmed by investigation of the textures with a λ-plate retarder between crossed polarizers. In the micrographs taken with a λ-plate (e.g., Figures 8d and S7, Supporting Information), the yellow and blue colors define the orientation of the high-index axis as tangential rather than radial within fans or "spherulites". Since the columns are known to be tangential, and the high-index axis parallel to the

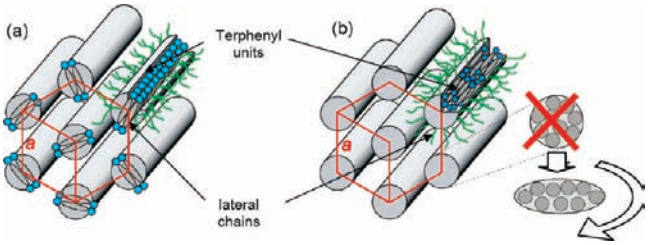

Figure 6. Alternative models of the arrangement of compounds **1** and **2** in the Col_{hex} phase: (a) terphenyl segments are perpendicular to the column and (b) terphenyls are parallel to the column axis; in this case the terphenyl cores of approximately 10 molecules should form the cross section of the column (for calculations see Table S10, Supporting Information), and a periodicity corresponding to the molecular length could arise if the glycerol groups register into distinct hydrogen-bonding networks; a circular column cross section is thought unlikely, as the lateral chains on the occluded molecules would not easily reach the surface of the bundle, hence flat bundles (ribbons) are envisaged, that are orientationally averaged; however, for simplicity, in the models the columns are shown as space- and time-averaged circular cylinders.[32]

terphenyl long axis, it follows that the terphenyls are coaxial with the columns.

The coaxial organization of the molecules could favor segregation of the aromatic units from the polar glycerol groups, leading to segmentation of the columns (see Figure 6b). To check for this possibility, IR spectra of compound **2a** were recorded between 50 and 170 °C. The spectra (Figure S5, Supporting Information) show a broad absorption between 3200 and 3600 cm^{-1} at all temperatures, confirming the presence of relatively large hydrogen-bonding clusters[42] in the LC state as well as in the crystalline and the isotropic liquid states. The presence of hydrogen-bonding networks in a structure with the terphenyls aligned parallel to the columns suggests that, within the columns, bundles of aromatic cores are separated by domains of glycerol units. This should lead to periodicity along the column axis corresponding to the length of bolaamphiphilic core (Figure 6b). Indeed, a periodicity of 2.23 nm, corresponding to the molecular length (L = 2.0−2.4 nm depending on the conformation of the glycerol groups) was found in the low-temperature phase ($R\bar{3}m$) occurring below the Col_{hex} phase of all compounds **1** (see next section). However, a 2.23 nm reflection was not observed in X-ray patterns of the high-temperature Col_{hex} phase, meaning that the segment positions are not correlated between the columns.

In spite of the lack of 3D long-range order, we can talk about the volume occupied by a column segment (the "unit cell") V_{cell}, calculated from a_{hex} and L = 2.2 nm. Dividing V_{cell} by the molecular volume gives about 10 molecules per cell for the Col_{hex} phases of all compounds **1** and **2** (see Table S10 of the Supporting Information). Thus, about 10 terphenyl units are arranged side-by-side in each bundle forming the aromatic column core. In order to enable the side chains on all molecules to have access to the column periphery, the local cross section of the aromatic column core is likely to be elliptical (ribbon-like), rather than circular (see Figure 6b, right); orientational averaging over space and time then gives rise to hexagonal symmetry and circular cores in the electron density maps Figures 3−5. The molecules of compounds **1** and **2** can adopt different conformations with respect to the orientation of the two swallow tail substituents to each other, an X- (chains at opposite sides) and a Π-shaped (chains at the same side), which are in equilibrium

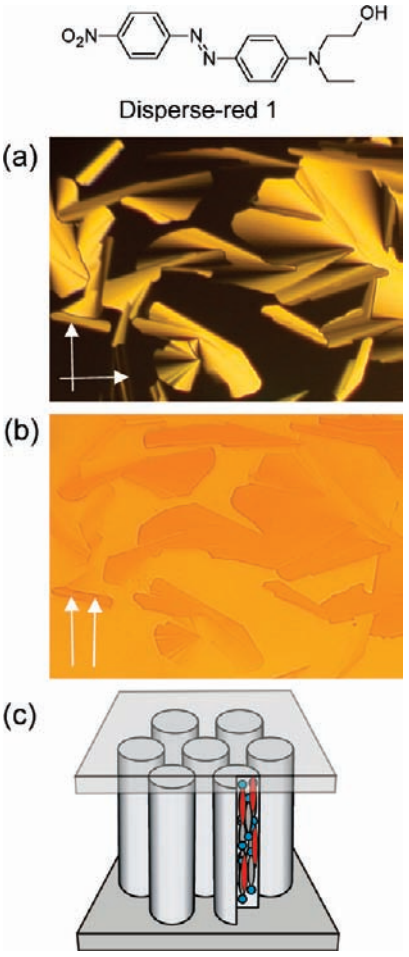

Figure 7. Optical microscopy of a mixture of compound **2a** and Disperse-red 1 (0.5 wt %, T = 140 °C): (a) spherulitic texture as seen between crossed polarizers; (b) same region as observed with parallel polarizers indicating the alignment of the dye with respect to the light beam as shown in (c).

(with other conformations) due to the rotation around the two aryl−aryl bonds of the terphenyl core. Nevertheless, it is likely that in the rod-bundles formed by on average 10 molecules in the cross section, the Π-shaped conformation is dominant as this allows a more efficient segregation of the flexible lateral chains from the rigid aromatics and a dense packing of the terphenyl moieties.

2.2. Correlated Rod-Bundles: Rhombohedral $R\bar{3}m$ Phase of Compounds ***1****.*

XRD pattern of compounds **1a**−**c** changes in the mesomorphic temperature range (at T = 150 °C for **1a**, at T = 130 °C for **1b**, and at 125 °C for **1c**, see Table 1), though there is no indication of any additional peak in the DSC curves (see Figure 8a) or of any change in texture in the whole mesomorphic temperature range (see Figure 8b and c). Only a continuous increase in birefringence takes place with decreasing temperature, signifying an increase of the orientational order parameter of the aromatics. In the powder XRD pattern of the Col_{hex} phase of compound **1c**, for example, an additional very weak diffraction peak, corresponding to d = 2.05 nm, appears at ca. 135 °C, which continuously increases in intensity upon further cooling (see Figure 9a). A number of additional *hkl* reflections can be observed in the GISAXS pattern of a highly oriented LC film

dx.doi.org/10.1021/ja110065r | *J. Am. Chem. Soc.* 2011, 133, 4906–4916

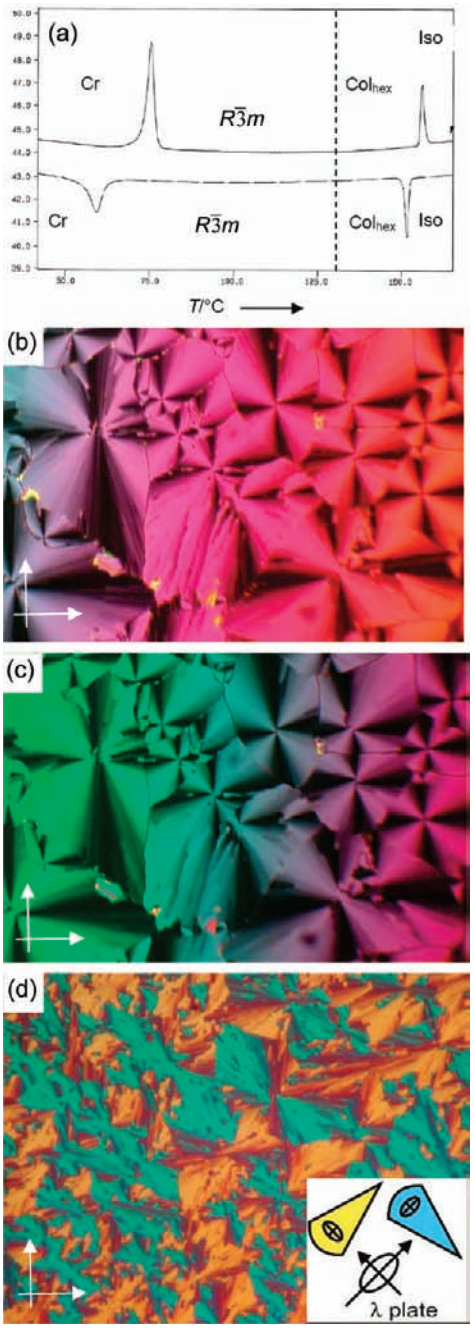

Figure 8. Compound **1c**: (a) DSC heating (solid line) and cooling curves (dashed line, rates: 10 K min^{-1}) and textures (crossed polarizers) as observed for: (b) the Col$_{hex}$ phase at T = 150 °C; (c) the $R\bar{3}m$ phase at T = 100 °C; (d) the Col$_{hex}$ phase at T = 150 °C with λ-plate retarder (different sample). The indicatrix orientation in the compensator and in the two orientations of the fans is shown in the inset; position of polarizer and analyzer are shown with white arrows.

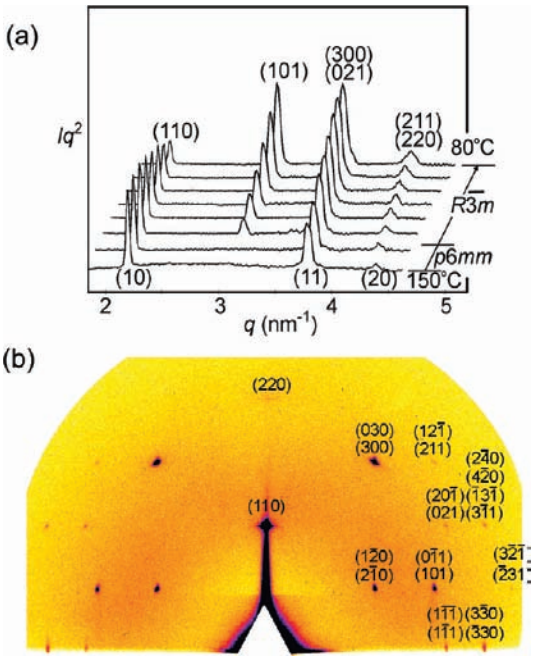

Figure 9. $R\bar{3}m$ phase of compound **1c**: (a) SAXS spectra (synchrotron source) recorded at decreasing temperatures showing the Col$_{hex}$−$R\bar{3}m$ transition indicated by the appearance of the (101) rhombohedral reflection; (hk) indices refer to Col$_{hex}$ and (hkl) to $R\bar{3}m$ phase using hexagonal coordinates. (b) GISAXS pattern of the $R\bar{3}m$ phase recorded at 110 °C with indices (mostly multiple) above the observed reflections; note that reflections (2−21) and (−22−1) are also superimposed on (3−30).

aligned on Si surface (Figure 9b). These were indexed on a rhombohedral lattice, space group $R\bar{3}m$, with lattice parameters a_{hex} = 5.87 nm, and c = 2.24 nm. The orientation is planar, as in the Col$_{hex}$ phase, with z-axis in the film plane.

The rhombohedral lattice results from the establishment of 3D register of the column segments. The c = 2.24 nm periodicity is well within the range of the bolaamphiphilic core length (L = 2.0−2.4). The absence of noticeable latent heat of the Col$_{hex}$−rhombohedral transition (Figure 8a) and the lack of change in the OH-stretching absorption in the IR spectrum, i.e., the lack of change in hydrogen-bonding (Figure S5, Supporting Information), suggest that segmented columns persist in the entire range studied, from the Col$_{hex}$ phase right into the isotropic liquid, albeit only with short-range order (see Figure 6b). In the 3D electron density map of the $R\bar{3}m$ phase of compound **1c** in Figure 10a and b, the red undulated cylinders, enclosing the low electron density areas, contain the column cores formed by the bolaamphiphilic units (terphenyls + glycerols). The alternation of aromatic and glycerol groups along these columns is in line with the undulation of the electron density along the columns. The projections of the undulating columns are arranged on a 2D hexagonal lattice, and there are three columns in a rhombic unit cell. In one unit cell each column contains one segment, i.e., a 10-molecule bundle, shifted along the z-direction by either 0, $c/3$ or $2c/3$, as represented in red, green, and yellow, respectively, in Figure 10c. Based on the lattice parameter a_{hex} of the $R\bar{3}m$ phase, the distance l between neighboring columns is 3.39 nm ($l = a_{hex}/3^{1/2}$), which is almost equal to the lattice parameter of the Col$_{hex}$ phase observed at higher temperatures (a_{hex} = 3.32 nm, see Table 1). This suggests that upon cooling through the phase transition the columns simply lock into longitudinal register without any prominent transverse displacement. The high electron density domains (blue, Figure 10a and b) enclose the regions with highest concentration of the fluorinated chains. In spite of having a lower fluorine content, the continuum surrounding these regions still has a higher electron density than the bolaamphiphilic column cores, meaning that the continuum still contains a mixture of R_H and R_F

dx.doi.org/10.1021/ja110065r |J. Am. Chem. Soc. 2011, 133, 4906–4916

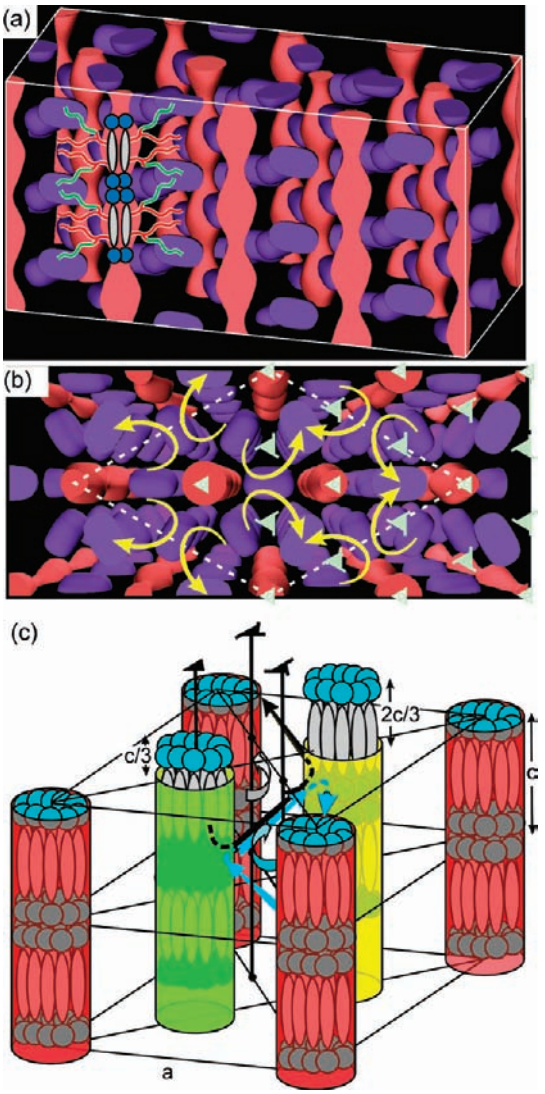

Figure 10. $R\bar{3}m$ phase of compound **1c**: (a and b) Oblique and top views of the reconstructed 3D electron density map obtained from the powder pattern at 120 °C; red = low density, in this map corresponding to the terphenyl and glycerol groups, including a portion of the alkyl segments of the side-chains); blue = high density (pure or nearly pure R_F groups); transparent continuum = mixed alkyl and R_F groups; schematic molecules are added in (a). In (b) symbols indicate location of three-fold rotation axes and 3_1 screw axes, while curved arrows show the helical relationship between R_F domains (each arrow connects three R_F domains shifted along z by $c/3$, $2/3c$, and c). (c) Bundles of molecular cores (terphenyl and glycerol groups) in the $R\bar{3}m$ phase (schematic); the green and yellow bundles are shifted along z by $1/3c$ and $2/3c$, respectively; the arrows indicate the action of two adjacent 3_1 axes on glycerol zones in adjacent columns. Black arrows follow a right-handed helix starting with $z = 0$ on the red column at rear left (indicated by dotted line, arrow hidden by green column) passing via the green ($z = c/3$) and yellow ($z = 2c/3$) columns and ending again on the starting red column at $z = c$. Similarly, the left-handed helix starts at the red column in the front, right and follows the blue arrows via the green and yellow back to the red column.

segments. In fact there is a slightly higher electron density spine in the center of the red undulated columns in Figure 10a and b, albeit less than in the high-temperature Col_{hex} phase, see Figure 5b. The intensification of the (101) diffraction peak

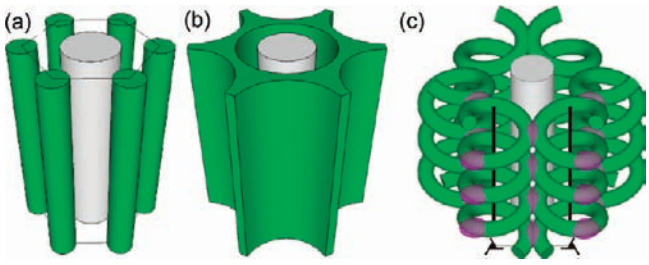

Figure 11. Different modes of organization of the R_F chains in the mesophases of compounds **1** and **2**: (a) in the Col_{hex} phase of **1c** and **2a**, (b) in the Col_{hex} phase of **2c**, and (c) in the rhombohedral $R\bar{3}m$ phase of **1c**; green: R_F-rich regions; gray: columns of the rod-bundles. The two helices in the front in (c) are decorated with purple blobs which represent the regions of highest R_F concentration.

with decreasing temperature (Figure 9a) is the result of a progressive increase in longitudinal register (positional order parameter) of the column segments, seen as increasing undulation amplitude of column cores in the electron density maps, see the effect of temperature on column undulation in Figure S8, Supporting Information.

It should be noted that the R_F domains are arranged on alternative right- and left-handed helices as indicated in Figure 10a and b. The helical structure results from the 3_1 screw axes inherent to $R\bar{3}m$ symmetry and is linked to the 1/3 shift of the individual columns as shown in Figure 10c, where the arrows trace the path between the glycerol zones of adjacent columns. These arrows follow a right- (black) and a left-handed (blue) 3_1 screw axis. The helical R_F regions appear on cooling through the Col_{hex}—$R\bar{3}m$ phase transition by deformation and condensation into blobs of the continuous straight R_F columns of the Col_{hex}/*p6mm* phase (see Figures 5b, blue column projections, and Figure 11a, green columns). These blobs appear as high electron density regions (blue/purple) in the electron density maps in Figure 10a and b and in the schematic in Figure 11c.

In relation to the helical arrangement of fluorine-rich domains we note that all compounds **1** comprise four sterogenic centers in the molecules, and they actually represent mixtures of diastereomers in racemic form. While overall the compounds and the structure are optically inactive, it is possible that a degree of enantiomeric separation develops on the local scale, as different isomers may fit better to helices of one or the other sense. While this is difficult to establish here, a related case of enantiomer separation into right- and left-handed helical columns has recently been reported in racemic liquid crystal helicenes.[43]

In contrast to compounds **1** no transition to a 3D ordered phase was observed for any of the compounds **2** with longer and more bulky lateral chains having two fluorinated branches. The reason might be that the shorter chains of compounds **1** allow a stronger coupling between the aromatic columns, which induces positional correlation between them. The intercolumnar interactions are weaker for compounds **2** due to the larger distances between the columns (a_{hex} = 3.7—4.5 nm compared to a_{hex} = 3.0—3.3 nm for compounds **1**).[44] Moreover, the side-by-side fixation of a fluorinated and a hydrocarbon chain in each of the swallow tail branches of compounds **1** may cause an increased tendency for segregation of R_F and R_H along z-axis and not just in the xy plane as in compounds **2**. The arrangements of R_F-rich domains in different phases of compounds **1** and **2** are schematically represented in Figure 11.

dx.doi.org/10.1021/ja110065r | *J. Am. Chem. Soc.* 2011, 133, 4906–4916

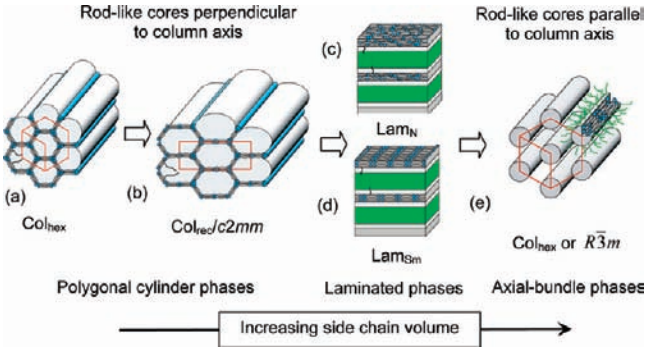

Figure 12. Sequence of different phase types formed by LC self-assembly of rod-like bolaamphiphiles with incompatible lateral and terminal chains, as seen upon increasing the size of the lateral chain(s): (a and b) polygonal cylinder phases; (c and d) Lam phases (rod-like cores parallel to the layer planes); and (e) axial-bundle phases.

SUMMARY AND CONCLUSIONS

In summary, new types of rod-like bolaamphiphiles with lateral swallow-tailed chains were synthesized, and new modes of LC self-assembly are reported with the aromatic rods grouped in bundles parallel to the column axis (axial-bundle columnar phases). Besides the polygonal cylinder phases (see for example Figure 12a and b) and the laminated phases (Figure 12c and d), these axial-bundle phases (Figure 12e) represent the third fundamental mode of self-assembly of ternary amphiphiles with (branched) lateral chains. Moreover, the axial-bundle phases represent a new type of columnar organization in general, where rod-like units are aligned parallel to the column axis and not across it as in columnar phases of polycatenar compounds[10,11] or rod-like mesogens with bulky end chains.[17−20] The bundles stack up longitudinally forming segmented ribbons of elliptical cross-section. The segmentation is due to the segregation of the aromatics from the terminal glycerol groups.[45] The ribbons are surrounded by the disordered swallow-tailed lateral chains. There are at least two distinct subtypes, one with 2D and the other with 3D periodicity, i.e., a hexagonal columnar phase in which the ribbons are rotationally averaged giving rise to hexagonal symmetry with no indication of long-range axial positional correlation between column segments (Col$_{hex}$)[30f,32] and a 3D mesophase where the periodicity along the columns locks into register giving a 3D phase with rhombohedral $R\bar{3}m$ symmetry,[46] in which the bundles are longitudinally shifted by $\pm 1/3$ molecular length between adjacent columns. Regarding the nature of the latter phase, although there is 3D long-range order in density fluctuations, we still regard it as LC, since there is no preferred position for individual molecules in the *x*,*y*-plane, hence the diffuse wide-angle X-ray scattering.[47]

The formation of a Col$_{hex}$ phase of axially aligned hard spherocylinders has been observed in early MC/MD simulations by Frenkel et al.[48] The 2D-to-3D transition observed for compounds **1**, and the fact that it appears to be second order, is also important from the theoretical point of view, and parallels can be drawn with the nematic−smectic A transition.[49]

With respect to the molecular structure, the compounds discussed here are related to the previously reported T-shaped amphiphiles which organize into honeycomb-type polygonal cylinder phases in which the cylinders adopt a rhombic, square, pentagonal, hexagonal (Col$_{hex}$, Figure 12a), or stretched hexagonal cross section (Col$_{rec}$/*c2mm*, Figure 12b).[29,30] Further increase in the lateral chain volume, either through adding extra atoms or by increasing the temperature, leads to a transition to lamellar phases where the bolaamphiphilic cores lie in the layer planes (Lam$_N$ and Lam$_{Sm}$, Figure 12c and d).[29,35,50] Further increasing the size of the lateral chains causes the Lam phases to transform to a new family of columnar LC phases with rod-bundle structure and 2D or 3D periodicity.[30f,32] With respect to the positions of rigid and flexible units, the mesophases at the extreme right and left of Figure 12 are the inverse of each other. The reversal of the position of flexible and rigid parts in these rigid/flexible amphiphiles is analogous to swapping the polar and nonpolar moieties in polar/apolar amphiphiles. In addition to this, a complete reorganization of the rod-like moieties with respect to the column long axis takes place in two steps. In the first step the polygonal cylinders of the honeycomb phases burst parallel to the hydrogen-bonding networks (i.e., perpendicular to the direction of the aromatic cores) resulting in the formation of layers (Lam phases).[30e] In the second step the layers of these Lam phases split parallel to the rod-like cores into infinite ribbons, giving rise to the axial-bundle phases.

The mesophases reported here are in some respect related to columnar mesophases of hairy rod main-chain polymers,[51] as the systems can be viewed as hydrogen-bonded supramolecular main-chain polymers[52] with the lateral chains as hairy side groups. However, in contrast to these polymers the molecules reported here are organized in bundles. Even some flexible and semiflexible polymers without lateral chains exhibit a main-chain columnar LC phase, but there again each chain forms a column of its own.[53] The hairy rod polymers[51,54,55] represent an important class of fluorescent and semiconducting organic materials for potential use in molecular electronics,[56] organic light-emitting diodes, organic transistors, and photovoltaic devices.[33,57] Hence, investigation of the low molecular weight molecules reported herein can provide clues concerning the controlled organization of these important functional materials by directed design of molecular tectons. More generally, these investigations have contributed to the general understanding of soft matter self-assembly and the molecular design principles required for generation of distinct types of complex phase morphologies.

ASSOCIATED CONTENT

Supporting Information. Synthesis procedures and analytical data, additional DSCs, textures, and XRD data. This material is available free of charge via the Internet at http://pubs.acs.org.

AUTHOR INFORMATION

Corresponding Author

g.ungar@sheffield.ac.uk, carsten.tschierske@chemie.uni-halle.de

ACKNOWLEDGMENT

This work, as part of the ESF EUROCORES Programme SONS, was supported by funds from the DFG, EPSRC, and the EC 6th Framework Programme, under contract ERAS-CT-2003-989409 and by the Fonds der Chemischen Industrie. G.U. also acknowledges the support from the WCU program through the National Research Foundation of Korea funded by the Ministry of Education, Science and Technology (R31-10013). M.P.

acknowledges the support by the Cluster of Excellence "Nanostructured Materials" and DFG (FG 1145). For help with the synchrotron experiments we thank Drs. Nick Terrill, Jen Hiller (beamline I22), Chris Nicklin, and Tom Arnold (I07) at Diamond and Drs. Oier Bikondoa, Simon Brown, and Paul Thompson (BM28−XMaS) at ESRF.

REFERENCES

(1) Steed, J. W.; Atwood, J. L. *Encyclopedia of Supramolecular Chemistry*; Marcel Dekker: New York, 2004.

(2) (a) Stewart, G. T. *Liq. Cryst.* **2003**, *30*, 541–557. (b) Stewart, G. T. *Liq. Cryst.* **2004**, *31*, 443–471. (c) Lydon, J. *Liq. Cryst. Today* **2006**, *15*, 1–10. (d) Lydon, J. *Liq. Cryst. Today* **2004**, *13*, 1–13. (e) Nakata, M.; Zanchetta, G.; Chapman, B. D.; Jones, C. D.; J. O. Cross, J. O.; Pindak, R.; Bellini, T.; Clark, N. A. *Science* **2007**, *318*, 1276–1279.

(3) Collings, P. J.; Hird, M. *Introduction to Liquid Crystals*; Taylor & Francis: London, 1997. Demus, D.; Goodby, J.; Gray, G. W.; Spiess, H.-W.; Vill, V. *Handbook of Liquid Crystals*, Wiley-VCH: Weinheim, Germany, 1998; Vol. 1−3. Pauluth, D.; Tarumi, K. *J. Mater. Chem.* **2004**, *14*, 1219–1227.

(4) Tschierske, C. *Annu. Rep. Prog. Chem., Sect. C: Phys. Chem.* **2001**, *97*, 191–267.

(5) Kato, T.; Mizoshita, N.; Kishimoto, K. *Angew. Chem., Int. Ed.* **2006**, *45*, 38–68. Ungar, G.; Zeng, X. *Soft Matter* **2005**, *1*, 95–106. Donnio, B.; Guillon, D. *Adv. Polym. Sci.* **2006**, *201*, 45–155. Saez, I. M.; Goodby, J. W. *Struct. Bonding (Berlin)* **2008**, *128*, 1–62.

(6) Chandrasekhar, S.; Sadashiva, B. K.; Suresh, K. A. *Pramana* **1977**, *9*, 471–480.

(7) Guillon, D. In *Structure and Bonding, Liquid Crystals II*; Mingos, D. M. P, Ed.; Springer: Berlin, Germany, 1999; Vol. 95, pp 41−82. Bushby, R. J.; Lozman, O. R. *Curr. Opin. Colloid Interface Sci.* **2002**, *7*, 343–354. Laschat, S.; Baro, A.; Steinke, N.; Giesselmann, F.; Hägele, C.; Scalia, G.; Judele, R.; Kapatsina, E.; Sauer, S.; Schreivogel, A.; Tosoni, M. *Angew. Chem., Int. Ed.* **2007**, *46*, 4832–4887.

(8) (a) Pisula, W.; Zorn, M.; Chang, J. Y.; Müllen, K.; Zentel, R. *Macromol. Rapid Commun.* **2009**, *30*, 1179–1202. (b) Wu, J.; Pisula, W.; Müllen, K. *Chem. Rev.* **2007**, *107*, 718–747. (c) Sergeyev, S.; Pisula, W.; Geerts, Y. H. *Chem. Soc. Rev.* **2007**, *36*, 1902–1929. (d) Pisula, W.; Feng, X.; Müllen, K. *Adv. Mater.* **2010**, *22*, 3634–3649.

(9) Chen, Z.; Stepanenko, V.; Dehm, V.; Prins, P.; Siebbeles, L. D. A.; Seibt, J.; Marquetand, P.; Engel, V.; Würthner, F. *Chem.—Eur. J.* **2007**, *13*, 436–449. Chen, Z.; Baumeister, U.; Tschierske, C.; Würthner, F. *Chem.—Eur. J.* **2007**, *13*, 450–465.

(10) Malthete, J.; Levelut, A. M.; Tinh, N. H. *J. Phys., Lett.* **1985**, *46*, L875–880. Tinh, N. H.; Malthete, J.; Destrade, C. *Mol. Cryst. Liq. Cryst. Lett.* **1985**, *2*, 133–138. Tinh, N. H.; Destrade, C.; Levelut, A. M.; Malthete, J. *J. Phys. (Paris)* **1986**, *47*, 553–557. Guillon, D.; Skoulios, A.; Malthete, J. *Europhys. Lett.* **1987**, *3*, 67–72. Destrade, C.; Tinh, N. H.; Roubineau, A.; Levelut, A. M. *Mol. Cryst. Liq. Cryst.* **1988**, *159*, 163–171. Levelut, A. M.; Malthete, J.; Destrade, C.; Tinh, N. H. *Liq. Cryst.* **1987**, *2*, 877–888. Nguyen, N. T.; Destrade, C.; Malthete, J. *Liq. Cryst.* **1990**, *8*, 797–811.

(11) Reviews:(a) Malthete, J.; Nguyen, H. T.; Destrade, C. *Liq. Cryst.* **1993**, *13*, 171–187. (b) Nguyen, H. T.; Destrade, C.; Malthete, J. *Adv. Mater.* **1997**, *9*, 375–388.(c) Nguyen, H. T.; Destrade, C.; Malthete, J. In *Handbook of Liquid Crystals*; Demus, D., Goodby, J., Gray, G. W., Spiess, H.-W., Vill, V., Eds.; Wiley-VCH: Weinheim, Germany, 1998; Vol. 2B, pp 865−900. (d) Gharbia, M.; Gharbi, A.; Nguyen, H. T.; Malthete, J. *Curr. Opin. Colloid Interface Sci.* **2002**, *7*, 312–325. (e) Bruce, D. W. *Acc. Chem. Res.* **2000**, *33*, 831–840.

(12) Originally the term "phasmidic" referred to rod-like molecules with three alkyl chains at both ends; "biforked" mesogens have two alkyl chains at both ends; now these molecules are generally named "polycatenar", where six-, five-, four-, and three-chain compounds are labeled hexa-, penta-, tetra-, and tricatenar, respectively; see ref 11c.

(13) Donnio, B.; Heinrich, B.; Gulik-Krzywicki, T.; Delacroix, H.; Guillon, D.; Bruce, D. W. *Chem. Mater.* **1997**, *9*, 2951–2965. Bruce, D. W. *Acc. Chem. Res.* **2000**, *33*, 831–840.

(14) Achard, M. F.; Tinh, N. H.; Richard, H.; Mauzac, M.; Hardouin, F. *Liq. Cryst.* **1990**, *84*, 533–544. Percec, V.; Heck, J.; Ungar, G. *Macromolecules* **1991**, *24*, 4957–4962.

(15) (a) Ungar, G.; Abramic, D.; Percec, V.; Heck, J. A. *Liq. Cryst.* **1996**, *21*, 73–86. (b) Sauer, C.; Diele, S.; Lindner, N.; Tschierske, C. *Liq. Cryst.* **1998**, *25*, 109–116.

(16) For bent polycatenar dithiolium salts formation of columnar phases was reported, where the organization of the molecules inside the columns is more driven by the amphiphatic feature of these salts than by the shape of the molecules: Artzner, F.; Veber, M.; Clerc, M.; Levelut, A. M. *Liq. Cryst.* **1997**, *23*, 27–33.

(17) Weissflog, W. in Demus, D.; Goodby, J.; Gray, G. W.; Spiess, H.-W.; Vill, V. *Handbook of Liquid Crystals*; Wiley-VCH: Weinheim, Germany, 1998; Vol. 2B, pp 835−863.

(18) Lee, M.; Cho, B.-K.; Zin, W.-C. *Chem. Rev.* **2001**, *101*, 3869–3892. Lee, M.; Yoo, Y.-S. *J. Mater. Chem.* **2002**, *12*, 2161–2168. Ryu, J.-H.; Cho, B.-K.; Lee, M. *Bull. Korean Chem. Soc.* **2006**, *27*, 1270–1282. Ryu, J.-H.; Lee, M. *Struct. Bonding (Berlin)* **2008**, *128*, 63–98.

(19) Nishikawa, E.; Samulski, E. T. *Liq. Cryst.* **2000**, *27*, 1463–1471.

(20) Guillevic, M.-A.; Bruce, D. W. *Liq. Cryst.* **2000**, *27*, 153–156. Lose, D.; Diele, S; Pelzl, G.; Dietzmann, E.; Weissflog, W. *Liq. Cryst.* **1998**, *24*, 707–717.

(21) Reddy, R. A.; Tschierske, C. *J. Mater. Chem.* **2006**, *16*, 907–961. Takezoe, H.; Takanishi, Y. *Jpn. J. Appl. Phys.* **2006**, *45*, 597–625.

(22) (a) Pegenau, A.; Hegmann, T.; Tschierske, C.; Diele, S. *Chem.—Eur. J.* **1999**, *5*, 1643–1660. (b) Pegenau, A.; Cheng, X. H.; Tschierske, C.; Göring, P.; Diele, S. *New J. Chem.* **1999**, *23*, 465–467. (c) Cheng, X. H.; Diele, S.; Tschierske, C. *Angew. Chem., Int. Ed.* **2000**, *39*, 592–595.

(23) Rosen, B. M.; Wilson, C. J.; Wilson, D. A.; Peterca, M.; Imam, M. R.; Percec, V. *Chem. Rev.* **2009**, *109*, 6275–6540.

(24) Borisch, K.; Diele, S.; Göring, P.; Kresse, H.; Tschierske, C. *J. Mater. Chem.* **1998**, *8*, 529–543. Fuchs, P.; Tschierske, C.; Raith, K.; Das, K.; Diele, S. *Angew. Chem., Int. Ed.* **2002**, *41*, 628–631. Cheng, X. H.; Das, K.; Diele, S.; Tschierske, C. *Langmuir* **2002**, *18*, 6521–6529. Kohlmeier, A.; Janietz, D. *Chem. Mater.* **2006**, *18*, 1483–1489.

(25) Seddon, J. M.; Templer, R. H. In *Handbook of Biological Physics*; Lipowsky, R., Sackmann, E., Eds.; Elsevier: Amsterdam, The Netherlands, 1995; Vol. 1, pp 97−160. Hassan, S.; Rowe, W.; Tiddy, G. J. T. In *Handbook of Applied Surface and Colloid Chemistry*; Holmberg, K., Ed.; Wiley: Chichester, U.K., 2002; Vol. 1, pp 465−508. Hyde, S. T. In *Handbook of Applied Surface and Colloid Science*; Holmberg, K., Ed.; Wiley: Chichester, U.K., 2002; Vol. 2, pp 299−332.

(26) (a) Tschierske, C. *J. Mater. Chem.* **1998**, *8*, 1485–1508. (b) Tschierske, C. *J. Mater. Chem.* **2001**, *11*, 2647–2671.

(27) Ostrovskii, B. I. In . *Liquid Crystals I*; Mingos, D. M. P., Ed.; Springer: Berlin, Germany, 1999; Vol. 94, pp 199−240.

(28) Donnio, B.; Heinrich, B.; Allouchi, H.; Kain, J.; Diele, S.; Guillon, D.; Bruce, D. W. *J. Am. Chem. Soc.* **2004**, *126*, 15258–15268.

(29) Tschierske, C. *Chem. Soc. Rev.* **2007**, *36*, 1930–1970.

(30) (a) Kölbel, M.; Beyersdorff, T.; Cheng, X. H.; Tschierske, C.; Kain, J.; Diele, S. *J. Am. Chem. Soc.* **2001**, *123*, 6809–6818. (b) Cheng, X. H.; Prehm, M.; Das, M. K.; Kain, J.; Baumeister, U.; Diele, S.; Leine, D.; Blume, A.; Tschierske, C. *J. Am. Chem. Soc.* **2003**, *125*, 10977–10996. (c) Cheng, X.-H.; Das, M. K.; Baumeister, U.; Diele, S.; Tschierske, C. *J. Am. Chem. Soc.* **2004**, *126*, 12930–12940. (d) Prehm, M.; Götz, G.; Bäuerle, P.; Liu, F.; Zeng, X.; Ungar, G.; Tschierske, C. *Angew. Chem., Int. Ed.* **2007**, *46*, 7856–7859. (e) Prehm, M.; Liu, F.; Baumeister, U.; Zeng, X.; Ungar, G.; Tschierske, C. *Angew. Chem., Int. Ed.* **2007**, *46*, 7972–7975. (f) Prehm, M.; Enders, C.; Anzahaee, M. Y.; Glettner, B.; Baumeister, U.; Tschierske, C. *Chem.—Eur. J.* **2008**, *14*, 6352–6368. (g) Cheng, X.; Dong, X.; Huang, R.; Zeng, X. B.; Ungar, G.; Prehm, M.; Tschierske, C. *Chem. Mater.* **2008**, *20*, 4729–4738. (h) Glettner, B.; Liu, F.; Zeng, X. B.; Prehm, M.; Baumeister, U.; Walker, M.; Bates, M. A.; Boesecke, P.; Ungar, G.; Tschierske, C. *Angew. Chem., Int. Ed.* **2008**, *47*, 9063–9066.

(31) (a) Chen, B.; Zeng, X.-B.; Baumeister, U.; Diele, S.; Ungar, G.; Tschierske, C. *Angew. Chem., Int. Ed.* **2004**, *43*, 4621–4625. (b) Chen, B.; Zeng, X.-B.; Baumeister, U.; Ungar, G.; Tschierske, C. *Science* **2005**,

307, 96–99. (c) Chen, B.; Baumeister, U.; Pelzl, G.; Das, M. K.; Zeng X.-B.; Diele, S.; Ungar, G.; Tschierske, C. *J. Am. Chem. Soc.* **2005**, *127*, 16578–16591. (d) Cook, A. G.; Baumeister, U.; Tschierske, C. *J. Mater. Chem.* **2005**, *15*, 1708–1721. (e) Liu, F.; Chen, B.; Baumeister, U.; Zeng, X.; Ungar, G.; Tschierske, C. *J. Am. Chem. Soc.* **2007**, *129*, 9578–9579. (f) Liu, F.; Chen, B.; Glettner, B.; Prehm, M.; Das, M. K.; Baumeister, U.; Zeng, X. B.; Ungar, G.; Tschierske, C. *J. Am. Chem. Soc.* **2008**, *130*, 9666–9667.

(32) Prehm, M.; Liu, F.; Zeng, X. B.; Ungar, G.; Tschierske, C. *J. Am. Chem. Soc.* **2008**, *130*, 14922–14923.

(33) Anthony, J. E. *Chem. Rev.* **2006**, *106*, 5028–5048. Kroon, R.; Lenes, M.; Hummelen, J. C.; Blom, P. W. M.; De Boer, B. *Polym. Rev.* **2008**, *48*, 531–582. Cheng, Y. J.; Yang, S.-H.; Hsu, C.-S. *Chem. Rev.* **2009**, *109*, 5868–5923. Kaeser, A.; Schenning, A. P. H. J. *Adv. Mater.* **2010**, *22*, 2985–2997.

(34) (a) Miyaura, N.; Yanagi, T.; Suzuki, A. *Synth. Commun.* **1981**, *11*, 513–519. (b) Hird, M.; Gray, G. W.; Toyne, K. J. *Mol. Cryst. Liq. Cryst.* **1991**, *206*, 187–204. (c) Miyaura, N.; Suzuki, A. *Chem. Rev.* **1995**, *95*, 2457–2483.

(35) Prehm, M.; Diele, S.; Das, M. K.; Tschierske, C. *J. Am. Chem. Soc.* **2003**, *125*, 614–615.

(36) Due to the presence of the stereogenic centers in the two glycerol groups, and for compounds **1** also at the branching points in the lateral chains, the investigated systems actually represent racemic mixtures of several stereoisomers.

(37) Immirzi, A.; Perini, B. *Acta Crystallogr., Sect. A* **1977**, *33*, 216–218.

(38) Enlarging the fluorinated segments also leads to mesophase stabilization in the series of compounds **2** (Table 2) due to the fluorophobic effect (see for example,Johannsson, G.; Percec, V.; Ungar, G.; Zhu, J. P. *Macromolecules* **1996**, *29*, 646–660); whereas there is no significant effect of elongation of the R_F segments on the mesophase stability of compounds **1** (Table 1) with only one fluorinated branch.

(39) For hexagonal cylinder phases of related *p*-terphenyl derivatives with only one lateral chain or with chains at opposite sides of the terphenyl unit parameters a_{hex} = 3.8−4.1 nm were found:Kieffer, R.; Prehm, M.; Glettner, B.; Pelz, K.; Baumeister, U.; Liu, F.; Zeng, X. B.; Ungar, G.; Tschierske, C. *Chem. Commun.* **2008**, 3861–3863.

(40) Calculation of the number of molecules in the unit cells (n_{cell}), defined by the hexagonal lattice parameter a_{hex} and assuming a height of the cell of h = 0.45 nm (corresponding to the lateral mean distance between the aromatic cores in such a hexagonal cylinder array) would amount only n_{cell} = 2.2 for all compounds (see Table S10 of the Supporting Information), which is too small for a hexagonal cylinder structure. Such a cylinder structure would require a number of at least n_{cell} = 3, which is the lowest limit for stable cylinder phases. In fact, values of n_{cell} around or above 6 were found for all previously reported Col_{hex} phases of T-shaped ternary amphiphiles (see refs 29 and 30a, b, f, and g), i.e., there are about two aromatic cores in the cross section of the cylinder walls; only X-shaped amphiphiles with lateral chains at opposite sides of an aromatic core form predominately single wall cylinders with slightly more than one (1.1−1.3) aromatic core in the cross section of the cylinder walls, i.e., n_{cell} is about four for the hexagonal honeycombs formed by these compounds.[39]

(41) Wang, Y.-J.; Carlisle, G. O. *J. Mater. Sci.: Mater. Electron.* **2002**, *13*, 173–178.

(42) (a) Frank, H. S.; Wen, W.-Y. *Disc. Farad. Soc.* **1957**, *24*, 133–140. (b) Bellamy, L. J.; Pace, R. L. *Spectrochim. Acta* **1966**, 525–534.(c) Kleeberg, H. In *Intermolecular Forces, An Introduction to Modern Methods and Results*; Huyskens, P. L., Luck, W. A. P., Zeegers-Huyskens, T., Eds.; Springer: Berlin, Germany, 1992; pp 251−280.

(43) Shcherbina, M. A.; Zeng, X. B.; Tadjiev, T.; Ungar, G.; Eichhorn, S. H.; Phillips, K. E. S.; Katz, T. J. *Angew. Chem., Int. Ed.* **2009**, *48*, 7837–7840.

(44) Only compound **2a** with the shortest swallow-tailed chains in this series shows an additional phase transition at T = 97 °C, but this transition is distinct from the 2D-to-3D transitions observed for compounds **1**, as it is associated with a significant transition enthalpy (ΔH = 4.8 kJ mol^{-1}, see Figure S3, Supporting Information). The precise structure of this mesophase M, though it is clearly a LC phase (maintenance of the diffuse wide angle scattering), has not yet been resolved.

(45) T-shaped rod-coil molecules with lateral coils but without terminal groups were also reported recently, however these molecules show a different self assembly behavior (stepped stripes) as there is no attractive end-to-end interaction, which is essential for the formation of the polygonal cylinder phases and the rod-bundle phases, see Hong, D.-J.; Lee, E.; Lee, J.-K.; Zin, W.-C.; Han, M.; Sim, E.; Lee, M. *J. Am. Chem. Soc.* **2008**, *130*, 14448–14449.

(46) A $R\bar{3}m$ phase was recently also observed for the organization of functionalized gold nanoparticles in a calamitc nematic matrix. In this case the 3D packing is provided by the optimization of the packing of the nanoparticles in the nematic director field: Zeng, X. B.; Liu, F.; Fowler, A. G.; Ungar, G.; Cseh, L.; Mehl, G. H. J.; Macdonald, E. *Adv. Mater.* **2009**, *21*, 1746–1750. An orthorhombic LC phase with columnar elements has been reported in dendrimers, space group *Pmna*: Rosen, B. M.; Peterca, M.; Huang, C.; Zeng, X. B.; Ungar, G.; Percec, V. *Angew. Chem., Int. Ed.* **2010**, *49*, 7002–7005.

(47) Pershan, P. S. *Structure of Liquid Crystal Phases*; World Scientific: Singapore, 1988.

(48) Veerman, J. A. C.; Frenkel, D. *Phys. Rev. A* **1991**, *43*, 4334–4343.

(49) de Genns, P. J.; Prost, J. *Physics of Liquid Crystals*; Oxford Science Publishers: Oxford, England, 1975.

(50) (a) Cheng, X. H.; Das, M. K.; Diele, S.; Tschierske, C. *Angew. Chem., Int. Ed.* **2002**, *41*, 4031–4035. (b) Prehm, M.; Cheng, X. H.; Diele, S.; Das, M. K.; C. Tschierske, C. *J. Am. Chem. Soc.* **2002**, *124*, 12072–1273. (c) Patel, N. M.; Dodge, M. R.; Zhu, M. H.; Petschek, R. G.; Rosenblatt, C.; Prehm, M.; Tschierske, C. *Phys. Rev. Lett.* **2004**, *92*, 015501. (d) Patel, N. M.; Syed, I. M.; Rosenblatt, C.; Prehm, M.; Tschierske, C. *Liq. Cryst.* **2005**, *32*, 55.

(51) Fu, K.; Sekine, N.; Sone, M.; Tokita, M.; Watanabe, J. *Polymer J.* **2002**, *34*, 291–297. Carbonnier, B.; Andreopoulou, A. K.; Pakula, T. J.; Kallitis, K. *Macromol. Chem. Phys.* **2005**, *206*, 66–76. Kim, L.; Arnt, T.; Atkins, E.; Tew, G. N. *Chem.—Eur. J.* **2006**, *12*, 2423–2427. Riala, P.; Andreopoulou, A.; Kallitsis, J.; Gitsas, A.; Floudas, G. *Polymer* **2006**, *47*, 7241–7250.

(52) Rieth, S.; Baddeley, C.; Badjic, J. D. *Soft Matter* **2007**, *3*, 137–154.*Supramolecular Polymers*, 2nd ed.; Ciferri, A., Ed.; Marcel Dekker, Inc.: New York, 2006; Hoogenboom, R.; Schubert, U. S. *Chem. Soc. Rev.* **2006**, *35*, 622–629. Rowan, S. J.; Mather, P. T. *Struct. Bonding (Berlin)* **2008**, *128*, 119–149.

(53) Ungar, G. *Polymer* **1993**, *34*, 2050–2059.

(54) Zheng, R.-Q.; Chen, E.-Q.; Cheng, S. Z. D.; Xie, F.; Yan, D.; He, T.; Percec, V.; Chu, P.; Ungar, G. *Macromolecules* **1999**, *32*, 3574–3582.

(55) Watanabe, J.; Sekine, N.; Nematsu, T.; Sone, M.; Kricheldorf, H. R. *Macromolecules* **1996**, *29*, 4816–4818.

(56) Petty, M. C. *Molecular Electronics. From Principles to Practice*; Wiley: New York, 2008. Funahashi, M.; Shimura, H.; Yoshio, M.; Kato, T. *Struct. Bonding (Berlin)* **2008**, *128*, 151–179.

(57) Pankaj, S.; Beiner, M. *Soft Matter* **2010**, *6*, 3506–3516. Kreyes, A.; Ellinger, S.; Landfester, K.; Defaux, M.; Ivanov, D. A.; Elschner, A.; Meyer-Friedrichsen, T.; Ziener, U. *Chem. Mater.* **2010**, *22*, 2079–2092.